Research paper

Cite as: Bhalke P, Pattath Sankaran P, Prabhu AN, Kadavigere R, Koteshwara P: Diagnostic cut-off values and grading of carpal tunnel syndrome by shear wave elastography at different tunnel locations correlated with gold standard nerve conduction study – a case-control study. J Ultrason 2025; 25: 17. doi: 10.15557/JoU.2025.0017.

Submitted: 04.02.2025
Accepted: 30.05.2025
Published: 30.06.2025

Diagnostic cut-off values and grading of carpal tunnel syndrome by shear wave elastography at different tunnel locations correlated with gold standard nerve conduction study – a case-control study

Prashat Bhalke[1], Priya Pattath Sankaran[1], Arvind N. Prabhu[2], Rajagopal Kadavigere[1], Prakashini Koteshwara[1]

[1] *Department of Radiodiagnosis, Kasturba Medical College, Manipal, Manipal Academy of Higher Education, Manipal, India*
[2] *Department of Neurology, Kasturba Medical College, Manipal, Manipal Academy of Higher Education, Manipal, India*

Corresponding author: Priya Pattath Sankaran; e-mail: priya.ps@manipal.edu

DOI: 10.15557/JoU.2025.0017

Keywords

ultrasound; shear wave elastography; carpal tunnel syndrome; nerve conduction study; median nerve

Abstract

Aim: The gold standard nerve conduction study for diagnosing carpal tunnel syndrome is often painful and has variable diagnostic accuracy. This study aimed to evaluate the diagnostic performance of shear wave elastography in correlation with nerve conduction study. **Material and methods:** A prospective case-control study was conducted on 50 participants (50 wrists), including 25 carpal tunnel syndrome cases diagnosed by nerve conduction study and 25 healthy controls. Shear wave elastography assessed the stiffness of the median nerve at three locations: outside the carpal tunnel, at the inlet, and at the outlet. Cross-sectional area measurements were also obtained using B-mode ultrasound. Receiver operating characteristic curves were used to evaluate diagnostic performance. **Results:** Shear wave elastography and cross-sectional area demonstrated high diagnostic accuracy for carpal tunnel syndrome, with a cut-off value of ≥63.5 kPa inside the tunnel (mean of inlet and outlet values) and a cross-sectional area cut-off of ≥0.08 cm² at the inlet of the tunnel offering optimal performance. While cross-sectional area provided high sensitivity, shear wave elastography showed superior specificity; their combination improved overall diagnostic accuracy. Shear wave elastography values did not significantly differ across carpal tunnel syndrome severity grades based on nerve conduction study (p >0.05). However, shear wave elastography at the tunnel inlet differentiated severe carpal tunnel syndrome from non-severe cases (p = 0.045), with a cut-off of ≥126 kPa predicting severe carpal tunnel syndrome with 100% sensitivity, 77% specificity, and an area under the receiver operating characteristic curve of 0.871. **Conclusions:** Shear wave elastography is a reliable, non-invasive modality for carpal tunnel syndrome diagnosis, offering excellent specificity, particularly when combined with cross-sectional area. Additionally, shear wave elastography at the tunnel inlet may help identify severe carpal tunnel syndrome, supporting timely clinical decision-making and prioritization of intervention.

Introduction

Carpal tunnel syndrome (CTS) is a neurological disorder characterized by compression of the median nerve within the carpal tunnel at the wrist, leading to sensory symptoms such as pain and paresthesia. The prevalence of CTS increases with age[1]. The estimated annual incidence of CTS ranges from 2.2 to 5.4 cases per 1,000 individuals in females and from 1.1 to 3 cases per 1,000 individuals in males[2]. One of the theories explaining the higher prevalence in females is that the cross-sectional area of the carpal tunnel is smaller in females than in males[3]. The compression of the median nerve results from elevated pressure within the carpal tunnel at the wrist, which arises from a multifactorial etiology. The most significant contributing factors include anatomical compression and inflammatory processes[4]. The diagnosis of CTS is primarily clinical, characterized by exclusive sensory symptoms in the regions innervated by the median nerve. Nerve conduction studies (NCS) and other diagnostic tests are used to confirm the diagnosis, assess the severity of CTS, and determine an appropriate treatment approach, whether surgical or non-surgical. Almost two-thirds of patients having milder form of the disease recover without the need for any surgical intervention[5]. The gold standard diagnostic test for CTS is NCS[6]. Patients with mild CTS symptoms achieve fa-

vorable results through nonsurgical treatment[7,8], whereas those diagnosed with moderate to severe CTS who show axonal loss on NCS are generally eligible for surgical decompression.

Material and methods

The study was conducted in the Department of Radiodiagnosis and Imaging in a tertiary care center, from April 2023 to August 2024. A total of 50 participants were enrolled and divided into two groups: 25 cases diagnosed with CTS based on NCS and 25 controls without clinical symptoms of CTS. The study excluded individuals who had previously undergone carpal tunnel release surgery, had a history of wrist fractures or surgeries, or presented with a bifid median nerve.

For each participant, the cross-sectional area (CSA) of the median nerve and stiffness of the median nerve were measured at three locations: outside the carpal tunnel, at the tunnel inlet, and at the tunnel outlet, using shear wave elastography (SWE). Ultrasound imaging was performed by an expert radiologist with 7 years of experience in radiology, including musculoskeletal ultrasound. Scans were conducted using a Philips EPIQ Elite ultrasound machine with a high-frequency ultrasound probe (EL18–4 MHz), utilizing the SWE settings provided by the manufacturer. The CSA of the median nerve was recorded using the free hand boundary-tracing approach in the axial plane, with the transducer held perpendicular to the nerve and with no additional strain, at the pronator quadratus level, representing the area outside the carpal tunnel; the proximal carpal row, indicating the inlet of the carpal tunnel; and the distal carpal row, corresponding to the outlet of the carpal tunnel. SWE measures shear waves generated in the transverse plane, which result from local stress and tissue displacement induced by perpendicular shear waves from the ultrasound probe[9,10]. This technique is considered a reliable and supportive tool for assessing increased median nerve stiffness in patients with CTS. Median nerve stiffness was assessed using the SWE setting provided in the ultrasound system. The median nerve was visualized in the longitudinal plane at the wrist level. Once stability was achieved, the ultrasound screen displayed a shear modulus map, known as a color-coded elastogram. In this elastogram, areas of high stiffness appeared red, soft tissues were represented by blue, and intermediate stiffness was indicated by green and yellow hues. Once the entire median nerve was adequately visualized with color mapping, the image was frozen, and three regions of interest (ROIs), each 3 mm in diameter, were placed at distinct anatomical locations. These included the pronator quadratus level, representing the area outside the carpal tunnel; the proximal carpal row, indicating the tunnel inlet; and the distal carpal row, corresponding to the outlet of the carpal tunnel. The ultrasound system automatically provided quantitative stiffness (elasticity) values in kilopascals (kPa) for each location (Fig. 1).

The ultrasound machine internally calculates the shear wave velocity (Cs) in meters per second (m/s) from the elastogram and derives the corresponding shear modulus, which quantifies tissue stiffness in kilopascals (kPa)[8]. Shear waves propagate more rapidly in stiffer tissues, reflecting the local elastic and viscoelastic properties of the median nerve[11–13].

Statistical methods

Data were coded in Microsoft Excel and analyzed using SPSS v23 (IBM Corp.). Group comparisons were performed using the independent *t*-test for normally distributed data and the Wilcoxon test for non-normally distributed data. The chi-squared test was used for categorical comparisons, with Fisher's exact test applied when expected frequencies were low. Correlations were assessed using Pearson's coefficient for normal and Spearman's rank correlation for non-normal data distributions. Statistical significance was set at $p < 0.05$. ROC analysis determined optimal cut-off values for continuous predictors, and diagnostic performance was evaluated in terms of sensitivity, specificity, PPV, NPV, and accuracy.

Results

Observations on CSA for diagnosis of CTS

CSA outside the tunnel in cases and controls

The mean (SD) of CSA outside tunnel was 0.10 cm^2 (0.03) for cases and 0.06 cm^2 (0.01) for controls. The CSA outside the tunnel for

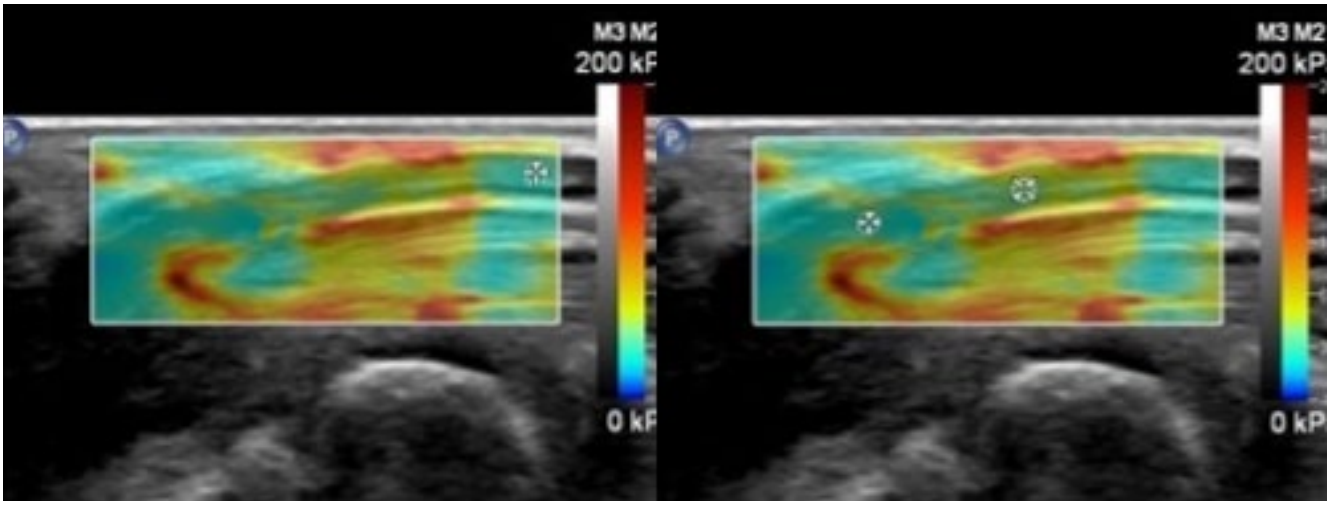

Fig. 1. *Placement of ROIs outside, at the inlet and at the outlet of the carpal tunnel on elastograms*

cases ranged from 0.06–0.18 cm^2, and for controls it ranged from 0.04–0.08 cm^2. There was a significant difference between the case and control groups in terms of CSA outside the tunnel (p <0.001), with the median CSA outside the tunnel being highest in cases. The strength of association (point-biserial correlation) was 0.62, indicating a large effect size.

The area under the ROC curve (AUROC) for CSA outside the tunnel in predicting cases from controls was 0.886 (95% CI: 0.801–0.972), thus demonstrating good diagnostic performance. At a cut-off of CSA outside the tunnel ≥0.08 cm^2, it predicted cases with a sensitivity of 80%, and a specificity of 80%.

CSA at the inlet of the tunnel in cases and controls

The mean (SD) of CSA at the inlet of the tunnel for cases was 0.12 cm^2 (0.04), and for controls it was 0.06 cm^2 (0.01). The CSA outside the tunnel for cases ranged from 0.06–0.26 cm^2 and for controls from 0.04–0.09 cm^2. There was a significant difference between cases and controls in terms of CSA at the inlet of the tunnel (p <0.001), with the median CSA at the inlet of the tunnel being highest in cases. The strength of association (point-biserial correlation) was 0.66, indicating a large effect size.

The AUROC for CSA at the inlet of the tunnel in predicting cases from controls was 0.958 (95% CI), thus demonstrating excellent diagnostic performance. At a cut-off of CSA at the inlet of the tunnel ≥0.08 cm^2, it predicted cases with a sensitivity of 96%, specificity of 84%, and diagnostic accuracy of 90%.

CSA at the outlet of the tunnel in cases and controls

The mean (SD) of CSA at the outlet of the tunnel for cases was 0.12 cm^2 (0.05), and for controls it was 0.07 cm^2 (0.01). The CSA at the outlet of the tunnel for cases ranged from 0.05–0.25 cm^2, and for controls it ranged from 0.04–0.1 cm^2. There was a significant difference between the case and control groups in terms of CSA at the outlet of the tunnel (p <0.001), with the median CSA at the outlet being highest in cases, and the strength of association (point-biserial correlation) was 0.63 (large effect size).

The AUROC for CSA at the outlet of the tunnel in predicting cases from controls was 0.915 (95% CI: 0.833–0.997), thus demonstrating excellent diagnostic performance. At a cut-off of CSA at the outlet of the tunnel ≥0.09 cm^2, it predicted cases with a sensitivity of 80% and a specificity of 92%.

CSA inside the tunnel in cases and controls

The CSA inside the tunnel is the mean of the CSA at the inlet and outlet of the tunnel.

The mean (SD) of CSA inside the tunnel for cases was 0.12 cm^2 (0.04), and for controls it was 0.06 cm^2 (0.01). The CSA inside the tunnel for cases ranged from 0.06–0.23 cm^2, and for controls it ranged from 0.04–0.1 cm^2. There was a significant difference between the case and control groups in terms of CSA inside the tunnel (p <0.001), with the median CSA inside the tunnel being highest in cases, and the strength of association (point-biserial correlation) was 0.67 (large effect size).

The AUROC for CSA inside the tunnel in predicting cases from controls was 0.946 (95% CI: 0.876–1.000), thus demonstrating excellent diagnostic performance. At a cut-off of CSA inside the tunnel ≥0.085 cm^2, it predicted cases with a sensitivity of 88% and a specificity of 96%.

Observations on SWE for the diagnosis of CTS

SWE outside the tunnel in cases and controls

The mean (SD) of SWE outside the tunnel for cases was 62.64 kPa (34.42), and for controls it was 32.54 kPa (8.83). The SWE outside the tunnel for cases ranged from 27.7–165 kPa, and for controls it ranged from 15–45.8 kPa. There was a significant difference between cases and controls in terms of SWE the outside tunnel (p <0.001), and the strength of association (point-biserial correlation) was 0.52 (large effect size).

The AUROC for SWE outside the tunnel in predicting cases from controls was 0.824 (95% CI: 0.711–0.937), thus demonstrating good diagnostic performance. At a cut-off of SWE outside the tunnel ≥45 kPa, it predicted cases with a sensitivity of 60% and a specificity of 92%.

SWE at the inlet of the tunnel in cases and controls

The mean (SD) of SWE at the inlet of tunnel for cases was 110.68 kPa (46.79), and for controls it was 42.32 kPa (14.29). The SWE at the inlet of the tunnel for cases ranged from 42.1–205 kPa, and for controls it ranged from 20–80 kPa. There was a significant difference between cases and controls in terms of SWE at the inlet of the tunnel (p <0.001), and the strength of association (point-biserial correlation) was 0.71 (large effect size).

The AUROC for SWE at the inlet of the tunnel in predicting cases from controls was 0.957 (95% CI: 0.909–1.000), thus demonstrating excellent diagnostic performance. At a cut-off of SWE at the inlet of the tunnel ≥60 kPa, it predicted cases with a sensitivity of 88% and a specificity of 92%.

SWE at the outlet of the tunnel in cases and controls

The mean (SD) of SWE at the outlet of the tunnel for cases was 90.31 kPa (45.75), and for controls it was 40.06 kPa (10.88). The SWE at the outlet of the tunnel for cases ranged from 31.1–224 kPa, and for controls it ranged from 13–68 kPa. There was a significant difference between cases and controls in terms of SWE at the outlet of the tunnel (p <0.001), and the strength of association (point-biserial correlation) was 0.61 (large effect size).

The AUROC for SWE at the outlet of the tunnel in predicting cases from controls was 0.904 (95% CI: 0.817–0.991), thus demonstrating excellent diagnostic performance. At a cut-off of SWE at the outlet of the tunnel ≥52.6 kPa, it predicted cases with a sensitivity of 80% and a specificity of 88%.

SWE inside the tunnel in cases and controls

The SWE inside the tunnel is the mean of the SWE at the inlet and outlet of the tunnel.

The mean (SD) of SWE inside the tunnel for cases was 100.50 kPa (40.50), and for controls it was 41.19 kPa (10.42). The SWE inside the tunnel for cases ranged from 36.6–204 kPa, and for controls it ranged from 18–63 kPa. There was a significant difference between cases and controls in terms of SWE inside the tunnel (p <0.001), and the strength of association (point-biserial correlation) was 0.72 (large effect size) (Fig. 2).

The AUROC for SWE inside the tunnel in predicting cases from controls was 0.957 (95% CI: 0.898–1.000), thus demonstrating excellent diagnostic performance. At a cut-off of SWE inside the tunnel ≥63.5 kPa, it predicted cases with a sensitivity of 88% and a specificity of 100% (Tab. 1).

Both CSA and SWE showed high diagnostic performance in the evaluation of carpal tunnel syndrome, with variation depending on the location of measurement. Among CSA parameters, the highest diagnostic accuracy was observed at the inlet of the carpal tunnel (AUROC = 0.958; 95% CI: 0.903–1.000; sensitivity: 96%; specificity: 84%; diagnostic accuracy: 90%) with a cut-off of ≥0.08 cm^2, predicting cases with a sensitivity of 96%, a specificity of 84%, and a diagnostic accuracy of 90%.

SWE assessments showed high diagnostic utility, with the best performance noted inside the tunnel (AUROC = 0.957; 95% CI: 0.898–1.000; sensitivity: 88%; specificity: 100%; diagnostic accuracy: 94%) at a cut-off of ≥63.5 kPa, predicting cases with a sensitivity of 88% and a specificity of 100%.

The combination of CSA and SWE measurements resulted in a significant improvement in diagnostic performance at all anatomical locations. The highest overall accuracy was observed for combined CSA+SWE measurements inside the tunnel (AUROC = 0.995; 95% CI: 0.984–1.000; sensitivity: 96%; specificity: 100%; diagnostic accuracy: 98%). At the tunnel inlet and outlet, the combined parameters also performed exceptionally well, with AUROC values of 0.992 and 0.982, respectively, and a diagnostic accuracy of 96% at both sites.

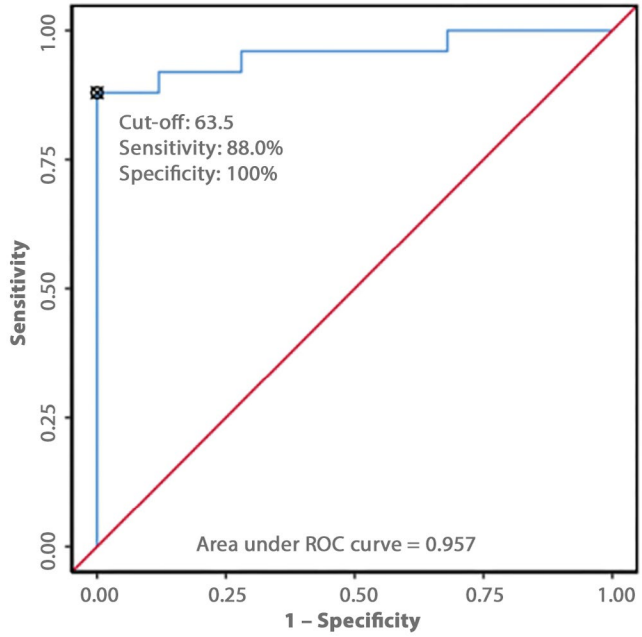

Fig. 2. *ROC curve analysis showing the diagnostic performance of shear wave elastography (SWE) inside the tunnel (mean of SWE at the inlet and outlet of the tunnel) in cases vs controls (n = 50)*

Even outside the tunnel, where individual SWE had the lowest accuracy, combining it with CSA improved the AUROC to 0.931 and increased diagnostic accuracy to 86%.

Observations on SWE for the grading of CTS

Shear wave elastography readings did not exhibit any significant variations in distinguishing between normal, mild, moderate, and severe NCS cases at any location (p >0.05). However, a significant

Tab. 1. Diagnostic performance of various parameters for diagnosing carpal tunnel syndrome

Predictor	AUROC	95% CI	*P*	Sn	Sp	PPV	NPV	DA
CSA outside tunnel	0.886	0.801–0.972	<0.001	80%	80%	80%	80%	80%
CSA inlet of tunnel	0.958	0.903–1	<0.001	96%	84%	86%	96%	90%
CSA outlet of tunnel	0.915	0.833–0.997	<0.001	80%	92%	91%	82%	86%
CSA inside tunnel	0.946	0.876–1	<0.001	88%	96%	96%	89%	92%
SWE outside tunnel	0.824	0.711–0.937	<0.001	60%	92%	88%	70%	76%
SWE inlet of tunnel	0.957	0.909–1	<0.001	88%	92%	92%	88%	90%
SWE outlet of tunnel	0.904	0.817–0.991	<0.001	80%	88%	87%	82%	84%
SWE inside tunnel	0.957	0.898–1	<0.001	88%	100%	100%	89%	94%
CSA+SWE outside tunnel	0.931	0.868–0.994	<0.001	72%	100%	100%	78%	86%
CSA+SWE inlet of tunnel	0.992	0.978–1	<0.001	96%	96%	96%	96%	96%
CSA+SWE outlet of tunnel	0.982	0.953–1	<0.001	92%	100%	100%	93%	96%
CSA+SWE inside tunnel	0.995	0.984–1	<0.001	96%	100%	100%	96%	98%

AUROC – area under ROC curve; CI – confidence interval; P – *p*-value; Sn – sensitivity; Sp – specificity; PPV – positive predictive value; NPV – negative predictive value; DA – diagnostic accuracy

difference was observed in predicting severe cases from non-severe cases exclusively at the inlet of the tunnel, which is crucial for patient selection for surgery[14].

SWE outside the tunnel in predicting severe cases

The mean (SD) SWE outside the tunnel for severe CTS cases was 56.33 kPa (18.77), and for non-severe CTS cases it was 63.50 kPa (36.25). The SWE outside the tunnel for severe CTS cases ranged from 36–73 kPa, while for non-severe cases it ranged from 27.7–165 kPa. There was no significant difference in predicting severe cases on SWE outside the tunnel (p = 1.000).

SWE at the inlet of the tunnel in predicting severe cases

The mean (SD) of SWE at the inlet of the tunnel for severe cases was 158.67 kPa (37.75), and for non-severe cases it was 104.14 kPa (44.63). The SWE at the inlet of the tunnel in severe cases ranged from 126–200 kPa, and in non-severe cases it ranged from 42.1–205 kPa. There was a significant difference in predicting NCS-severe cases in terms of SWE at the inlet of the tunnel (p = 0.045), and the strength of association (point-biserial correlation) was 0.39 (large effect size) (Fig. 3).

The AUROC for SWE at the inlet of the tunnel in predicting severe from non-severe cases was 0.871 (95% CI: 0.723–1.000), thus demonstrating good diagnostic performance. At a cut-off of SWE at the inlet of the tunnel ≥126 kPa, it predicted severe cases with a sensitivity of 100% and a specificity of 77%.

SWE at the outlet of the tunnel in predicting severe cases

The mean (SD) of SWE at the outlet of the tunnel in severe cases was 124.67 kPa (58.53), and in non-severe cases it was 85.63 kPa (43.30). The SWE at the outlet of the tunnel for severe cases ranged from 86–192 kPa, and for non-severe cases it ranged from 31.1–224 kPa. There was no significant difference between the groups in terms of SWE at the outlet of the tunnel (p = 0.259).

SWE inside the tunnel in predicting severe cases

The mean (SD) of SWE inside the tunnel for severe cases was 141.67 kPa (47.82), and for the non-severe group it was 94.88 kPa (37.17). The SWE inside the tunnel for severe cases ranged from 106–196 kPa, and for non-severe cases it ranged from 36.6–204 kPa. There was no significant difference in predicting severe from non-severe cases in terms of SWE inside the tunnel (p = 0.107) (Fig. 4, Fig. 5, Fig. 6).

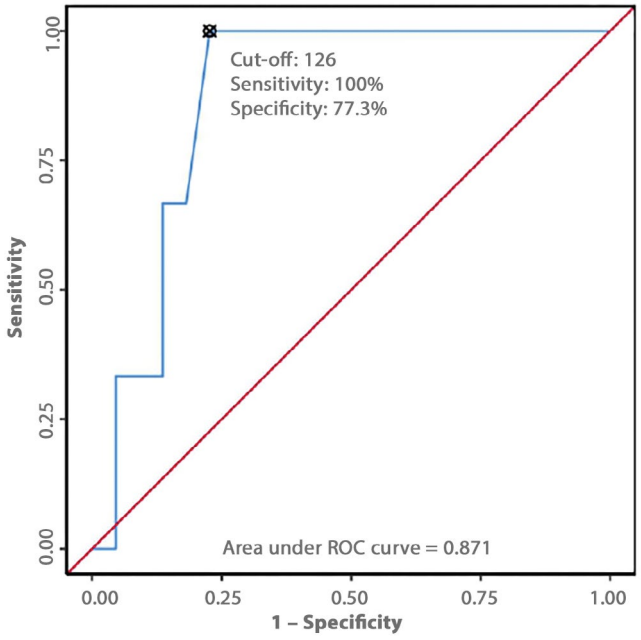

Fig. 3. *ROC curve analysis showing the diagnostic performance of shear wave elastography at the inlet of the tunnel in predicting severe carpal tunnel syndrome (n = 25)*

Discussion

This study highlights the diagnostic efficacy of both cross-sectional area (CSA) and shear wave elastography (SWE) in evaluating carpal tunnel syndrome (CTS), with findings that are consistent with and build upon previous research.

CSA measurements

The cross-sectional area of the median nerve is a well-established ultrasound parameter for diagnosing CTS. The present study shows

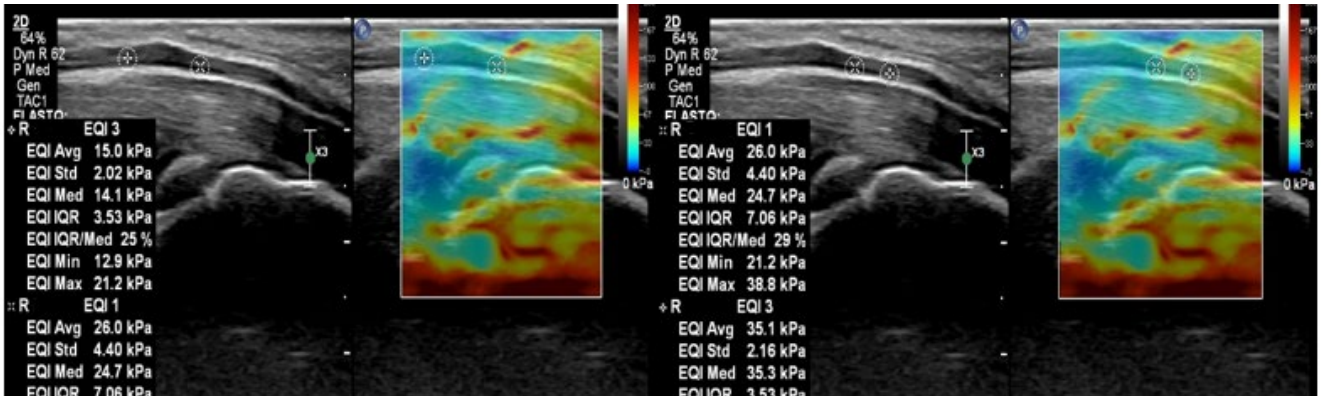

Fig. 4. *Shear wave elastography of a normal subject*

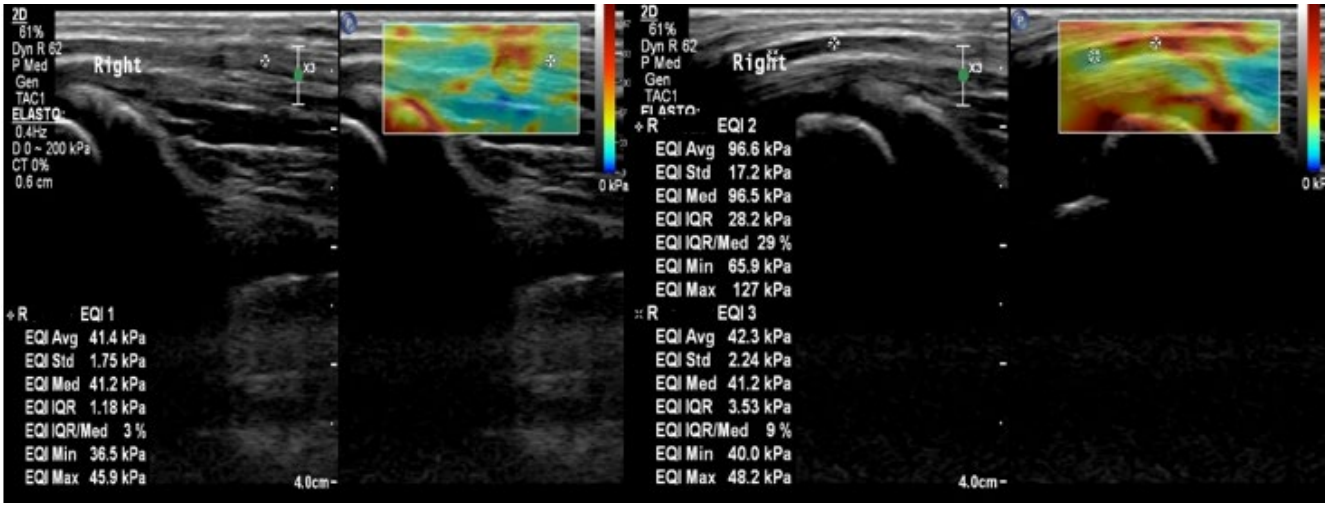

Fig. 5. *Shear wave elastography of a subject with moderate carpal tunnel syndrome*

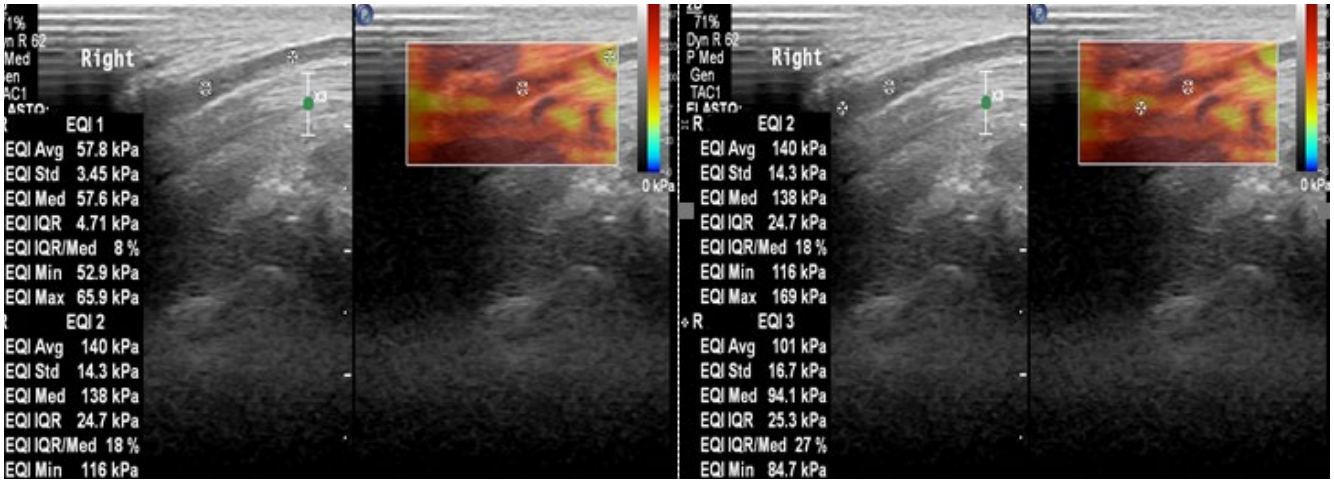

Fig. 6. *Shear wave elastography of a subject with severe carpal tunnel syndrome*

that the CSA at the inlet of the carpal tunnel demonstrated the highest diagnostic accuracy, with an AUROC of 0.958, sensitivity of 96%, and specificity of 84% at a cut-off of ≥0.08 cm^2. These findings are in agreement with those of Kantarci *et al.*[15], who demonstrated that CSA measurements correlate significantly with clinical and NCS findings in CTS patients. Mohammadi *et al.*[16] also reported a CSA cut-off of 0.07 cm^2, with a sensitivity and specificity of 88.8% and 88.4%, respectively. Park *et al.*[17] further observed significantly higher CSA values in CTS patients compared to controls, confirming its diagnostic value.

SWE measurements

Shear wave elastography is a newer, non-invasive technique that provides quantitative assessment of tissue stiffness. In the present study, SWE inside the tunnel (mean of inlet and outlet values) showed excellent diagnostic performance, with an AUROC of 0.957, sensitivity of 88%, and specificity of 100% at a cut-off of ≥63.5 kPa. These results echo those of Kantarci *et al.*[15], who reported increased stiffness in CTS patients compared to healthy individuals. Mohammadi *et al.*[16] also found a median nerve stiffness cut-off of 33.9 kPa with a sensitivity of 90.28% and specificity of 88.4%. Park *et al.*[17] reported significantly higher SWE values in CTS patients versus controls. Xin *et al.*[18] also demonstrated higher SWE values in hemodialysis patients with CTS, further supporting the reliability of elastographic techniques across diverse patient populations.

Combined CSA and SWE

The combination of CSA and SWE yielded superior diagnostic performance compared to either parameter alone. The highest diagnostic accuracy was observed inside the tunnel with combined CSA+SWE measurements (AUROC = 0.995, sensitivity = 96%, specificity = 100%, accuracy = 98%). This reflects the synergistic potential of combining morphological and biomechanical data, emphasizing the benefits of a multiparametric evaluation.

SWE for CTS severity grading

Although the findings of the present study indicated that SWE was not significantly different across all severity grades of CTS, SWE at the inlet of the tunnel was able to significantly differentiate severe CTS cases from non-severe ones (p = 0.045), with an AUROC of 0.871 at a cut-off of ≥126 kPa. This aligns with the findings by Mo-

hammadi *et al.*[16], who noted that SWE was more effective at distinguishing mild CTS from healthy controls but less so among moderate and severe cases. Tezcan *et al.* [19] also reported the potential of SWE to reflect severity in autoimmune-related CTS; however, variability in its correlation with NCS severity remains a limitation for broader clinical applications.

Limitations

The ultrasound technique is operator-dependent, making it susceptible to interpretive errors. Standardized protocols for performing elastography are necessary to improve consistency. Further prospective studies with larger sample sizes are needed to validate these findings.

Conclusions

The present study supports the utility of shear wave elastography (SWE) and cross-sectional area (CSA) of the median nerve as a non-invasive and reliable diagnostic tool for carpal tunnel syndrome (CTS), offering high diagnostic accuracy and clinical applicability. A SWE cut-off value of ≥63.5 kPa measured inside the tunnel (mean of inlet and outlet) and a CSA cut-off of ≥0.08 cm^2 at the inlet of the tunnel were identified as the optimal parameters for diagnosing CTS.

While CSA demonstrated high sensitivity and SWE provided superior specificity, their combination significantly improved diagnostic performance, particularly when measurements were obtained inside the carpal tunnel, achieving near-perfect diagnostic accuracy.

SWE values did not show statistically significant differences across the full spectrum of CTS severity as defined by nerve conduction studies (NCS), including normal, mild, moderate, and severe categories (p >0.05). However, SWE at the inlet of the carpal tunnel demonstrated a significant ability to distinguish severe CTS cases from non-severe ones (p = 0.045), with a large effect size (point-biserial correlation = 0.39). At a cut-off value of ≥126 kPa, SWE at the inlet predicted severe CTS with 100% sensitivity, 77% specificity, and an AUROC of 0.871 (95% CI: 0.723–1.000), indicating good diagnostic performance.

These findings highlight the diagnostic relevance of SWE at the tunnel inlet as a potential sonographic marker for identifying severe CTS, which may aid in surgical decision-making and prioritization of patients for intervention.

Conflict of interest

The authors do not report any financial or personal connections with other persons or organizations which might negatively affect the contents of this publication and/or claim authorship rights to this publication.

Author contributions

Original concept of study: PB, PPS. Writing of manuscript: PB. Analysis and interpretation of data: PB. Final acceptation of manuscript: PPS, RK, PK. Collection, recording and/or compilation of data: PB, PPS, ANP. Critical review of manuscript: PPS, RK, PK.

References

1. Pourmemari MH, Heliövaara M, Viikari-Juntura E, Shiri R: Carpal tunnel release: Lifetime prevalence, annual incidence, and risk factors. Muscle Nerve 2018; 58: 497–502. doi: 10.1002/mus.26145.
2. Atroshi I, Englund M, Turkiewicz A, Tägil M, Petersson IF: Incidence of physician-diagnosed carpal tunnel syndrome in the general population. Arch Intern Med 2011; 171: 943–944. doi: 10.1001/archinternmed.2011.203.
3. Keir PJ, Rempel DM: Pathomechanics of peripheral nerve loading. Evidence in carpal tunnel syndrome. J Hand Ther Off J Am Soc Hand Ther 2005; 18: 259–269. doi: 10.1197/j.jht.2005.02.001.
4. Bland JD: Carpal tunnel syndrome. Curr Opin Neurol 2005; 18: 581–585. doi: 10.1097/01.wco.0000173142.58068.5a.
5. Jablecki CK, Andary MT, Floeter MK, Miller RG, Quartly CA, Vennix MJ, Wilson JR; American Association of Electrodiagnostic Medicine; American Academy of Neurology; American Academy of Physical Medicine and Rehabilitation: Practice parameter: Electrodiagnostic studies in carpal tunnel syndrome. Report of the American Association of Electrodiagnostic Medicine, American Academy of Neurology, and the American Academy of Physical Medicine and Rehabilitation. Neurology 2002; 58: 1589–92. doi: 10.1212/wnl.58.11.1589.
6. Aroori S, Spence RA: Carpal tunnel syndrome. Ulster Med J 2008; 77: 6–17.
7. McClure P: Evidence-based practice: an example related to the use of splinting in a patient with carpal tunnel syndrome. J Hand Ther 2003; 16: 256–263. doi: 10.1016/s0894-1130(03)00043-7.
8. Kaplan SJ, Glickel SZ, Eaton RG: Predictive factors in the non-surgical treatment of carpal tunnel syndrome. J Hand Surg Br 1990; 15: 106–108. doi: 10.1016/0266-7681_90_90061-8.
9. Bercoff J, Tanter M, Fink M: Supersonic shear imaging: a new technique for soft tissue elasticity mapping. IEEE Trans Ultrason Ferroelectr Freq Control 2004; 51: 396–409. doi: 10.1109/tuffc.2004.1295425. Erratum in: IEEE Trans Ultrason Ferroelectr Freq Control 2020; 67: 1492–1494. doi: 10.1109/TUFFC.2020.2973565.
10. Li Y, Snedeker JG: Elastography: modality-specific approaches, clinical applications, and research horizons. Skeletal Radiol 2011; 40: 389–397. doi: 10.1007/s00256-010-0918-0.
11. Klauser AS, Miyamoto H, Bellmann-Weiler R, Feuchtner GM, Wick MC, Jaschke WR: Sonoelastography: musculoskeletal applications. Radiology. 2014; 272: 622–633. doi: 10.1148/radiol.14121765.
12. Drakonaki EE, Allen GM, Wilson DJ: Ultrasound elastography for musculoskeletal applications. Br J Radiol 2012; 85: 1435–1445. doi: 10.1259/bjr/93042867.
13. Li Y, Snedeker JG: Elastography: modality-specific approaches, clinical applications, and research horizons. Skeletal Radiol 2011; 40: 389–397. doi: 10.1007/s00256-010-0918-0.
14. Sonoo M, Menkes DL, Bland JDP, Burke D: Nerve conduction studies and EMG in carpal tunnel syndrome: Do they add value? Clin Neurophysiol Pract 2018; 3: 78–88. doi: 10.1016/j.cnp.2018.02.005.
15. Kantarci F, Ustabasioglu FE, Delil S, Olgun DC, Korkmazer B, Dikici AS *et al.*: Median nerve stiffness measurement by shear wave elastography: a potential sonographic method in the diagnosis of carpal tunnel syndrome. Eur Radiol 2014; 24: 434–40. doi: 10.1007/s00330-013-3023-7.
16. Mohammadi A, Afshar A, Mirza-Aghazadeh-Attari M, Mokhtari SAS: Application of shear wave elastography and median nerve cross-section area in the diagnosis and staging of carpal tunnel syndrome: a case-control study. Pol J Radiol 2021; 86: e638–e643. doi: 10.5114/pjr.2021.111437.
17. Park EJ, Hahn S, Yi J, Shin KJ, Lee Y, Lee HJ: Comparison of the diagnostic performance of strain elastography and shear wave elastography for the diagnosis of carpal tunnel syndrome. J Ultrasound Med 2021; 40: 1011–1021. doi: 10.1002/jum.15478.
18. Xin H, Hu HY, Liu B, Liu X, Li X, Li J: Ultrasound elastographic evaluation of the median nerve in hemodialysis with carpal tunnel syndrome. J Med Ultrason (2001) 2017; 44: 123–131. doi: 10.1007/s10396-016-0733-x.
19. Tezcan EA, Levendoglu F, Durmaz MS, Batur EB, Gezer IA, Erol K: Utility of shear wave elastography for diagnosing carpal tunnel syndrome with psoriatic arthritis. Ir J Med Sci 2024; 193: 977–985. doi: 10.1007/s11845-023-03512-5.